WIND LOADS ON LARGE INDUSTRIAL-TYPE BUILDINGS

John Ginger[1] John Holmes[2] and Heath Rodgers[1]

1) Cyclone Structural Testing Station, School of Engineering, James Cook University Townsville
2) Department of Mechanical Engineering, Monash University and JDH Consulting

INTRODUCTION

Large, low-rise buildings with spans greater than 30m and lengths exceeding 100m are often used for bulk storage of materials. The structural systems of such large buildings generally consist of portal or pin-jointed frames, usually spaced evenly at the mid section and closer together at the gable-ends. Cladding is attached to roof purlins and wall girts, which are fixed to these frames. Cross bracing between the end frames resist longitudinal (ie. in direction of ridgeline) wind loads. Design wind loads on the cladding and primary structure of such buildings may be determined using data in wind load standards (ie. AS 1170.2 (1989)).

An early study by Howe (1952) in smooth uniform flow identified the significant effect of aspect ratio (ie. AR = length, *b* / span, *d*) on wind pressures at the ends of low-rise buildings. More recently, studies on such buildings, in boundary-layer flows, by Kanda and Maruta (1993), Holmes (1998) and Ginger and Holmes (2001), found that an increase in aspect ratio resulted in increased suction pressures on the leeward roof and wall, especially on buildings with steep roof slopes. These pressures were significantly underestimated by AS 1170.2 (1989). AS/NZS 1170.2 (2001) attempts to overcome this shortcoming by increasing the magnitude of pressure coefficients on the leeward slopes of steep roof buildings. This paper summarises results from wind tunnel studies carried out on a range of large buildings at James Cook University.

WIND TUNNEL TESTS

The wind tunnel tests were carried out in the 2.0m high × 2.5m wide × 22m long Boundary Layer Wind Tunnel at the School of Engineering at James Cook University. Tests were carried out on the four building configurations shown in Figs. 1 to 4 and described in Table 1, at length scales of 1/200 and 1/300. Building configuration Nos. 1, 2 and 3 were tested in a simulated terrain category 2 while configuration No. 4 was tested in simulated terrain category 3 boundary layer approach flows (as per AS/NZS 1170.2 (2001)).

Table 1 Test building configurations and specifications

Config. No.	Roof Pitch (°)	Span (d), m	Mid roof height, m	Total height, m	Length (b), m	Aspect Ratio (b/d)
1-Fig 1	35	40	22	29	96, 160, 240	2.4, 4, 6
2-Fig 2	50	50	15	29.8	150, 200, 250, 300, 350, 400	3, 4, 5, 6, 7, 8
3-Fig 3	Curved	45	22.1	29.1	108, 225, 360	2.4, 5, 8
4-Fig 4	15	80	20.4	25.7	108, 240, 350	1.35, 3, 4.35

External pressures on the wall and roof panels were obtained for approach wind directions (θ) of -90° to 90° at intervals of 15°. Pressure taps were connected to Honeywell pressure transducers via Scanivalves and a calibrated tube and restrictor system. The pressure signals were low-pass filtered at a frequency of 250Hz, and sampled at 500Hz for 24secs for a single run. The pressures were analysed to give mean, standard deviation, maximum and minimum pressure coefficients as;

$$C_{\overline{p}} = \overline{p}/(\tfrac{1}{2}\rho\overline{U}_h^2), \quad C_{\sigma_p} = \sigma_p/(\tfrac{1}{2}\rho\overline{U}_h^2), \quad C_{\hat{p}} = \hat{p}/(\tfrac{1}{2}\rho\overline{U}_h^2) \text{ and } \quad C_{\breve{p}} = \breve{p}/(\tfrac{1}{2}\rho\overline{U}_h^2)$$

where, $\frac{1}{2}\rho\overline{U}_h^2$ is the mean dynamic pressure at height h, the average roof level.

The results were obtained from averaging the data from five separate runs. The correlation coefficients between pressures on each pair of panels on selected frame tributaries on some building configurations were also determined.

PRESSURE DISTRIBUTIONS

Measured pressure coefficients for $\theta = 45°$ and, 90° and -90° on the tributary of the second frame from the gable-end (ie. Frame B) on building configuration No 1, of AR = 6 and 4 are shown in Figures 5 and 6 respectively, along with peak pressure coefficients C_{peak} derived from AS1170.2. The peak (positive on windward half and negative on leeward half) pressure coefficients for $\theta = 45°$, on Frame B of building configurations 1, 2, 3 and 4 of varying AR are shown in Figures 7, 8, 9 and 10 respectively. Revised data in AS/NZS 1170.2 (2001) on the leeward roof and wall on the steep pitch, planar roof buildings of AR greater than 3, for $\theta = 0°$ gives a better representation of peak suction pressures than the data in AS1170.2 (1989).

STRUCTURAL LOAD EFFECTS

Based on a typical 3-pin frame system used in storage sheds, the knee and centre rafter bending moments (M_K and M_C) and horizontal (H) and vertical (V) reactions at the base of the second frame from the gable-end of building configuration No 1 are analysed in this section. The bending moments and horizontal and vertical reactions are non-dimensionalised as $C_M = M/(\frac{1}{2}\rho\overline{U}_h^2 d^2 w)$, $C_H = H/(\frac{1}{2}\rho\overline{U}_h^2 h_f w)$ and $C_V = V/(\frac{1}{2}\rho\overline{U}_h^2 dw)$ respectively, where w is the width of the tributary area and h_f is the height of the frame. Table 2 shows peak wind load effects for $\theta = 45°$ and $\theta = 90°$, derived from the "covariance integration" method of Holmes and Best (1981) and compared with that derived from AS/NZS 1170.2 (2001). Generally good agreement is seen, by using values given in AS/NZS 1170.2 (2001)

Table 2 Wind load effects on Building configuration No. 1 Frame B versus aspect ratio

Load Effect Coefficient	AR	Wind tunnel	AS/NZS1170.2 (2001)	Load Effect Coefficient	AR	Wind tunnel	AS/NZS1170.2 (2001)
		$\theta = 45°$	$\theta = 0°$			$\theta = 45°$	$\theta = 0°$
C_{MK}	2.4	0.094/-0.062	0.099/-0.084	C_H	2.4	-1.10	-1.21
	4	0.121/-0.073	0.105/-0.089		4	-1.36	-1.27
	6	0.139/-0.081	0.117/-0.097		6	-1.52	-1.39
C_{MC}	2.4	0.072/-0.089	0.089/-0.100				
	4	0.082/-0.123	0.091/-0.109			$\theta = 90°$	$\theta = 90°$
	6	0.089/-0.146	0.097/-0.125	C_V	6	-0.92	-0.98

CONCLUSIONS

Wind tunnel studies were carried out to determine pressure distributions and wind load effects on large low-rise buildings with varying roof shapes and aspect ratios. The following conclusions were reached:

- Large mean and peak suction pressure coefficients measured on the leeward half of the roof and wall near the windward gable-end, of the steep pitch gable roof buildings for oblique approach winds (ie. $\theta = 45°$) increase in magnitude with increasing aspect ratio.
- There is less variation with aspect ratio for buildings with a low pitched gable roofs and curved roofs

REFERENCES

Australian Standard SAA Loading Code Part 2 Wind Loads AS1170.2 (1989). Revised as Draft Structural design – General requirements and design actions, Wind actions AS/NZS 1170.2 (2001)

Ginger, J. D. and Holmes, J. D., "Wind loads on long low-rise buildings", Accepted for publication in VAPSSEWE Conference Kyoto Japan (2001)

Holmes, J. D. and Best, R. J., "An Approach to the determination of wind load effects on low-rise buildings", Journal of Wind Engineering & Industrial Aerodynamics, Vol. 7, 273-287, (1981)

Holmes, J. D., "Wind loads on the frames of large bulk-storage sheds", 7th Australasian Wind Engineering Society Workshop, Auckland NZ, October, (1998)

Howe, J.W., "Wind pressure on elementary building forms evaluated by model tests", Civil Engineering (ASCE), May, pp 42-46, (1952)

Kanda, M. and Maruta, E., "Characteristics of fluctuating wind pressure on long low-rise buildings with gable roofs", Journal of Wind Engineering & Industrial Aerodynamics, Vol. 50, 173-182, (1993)

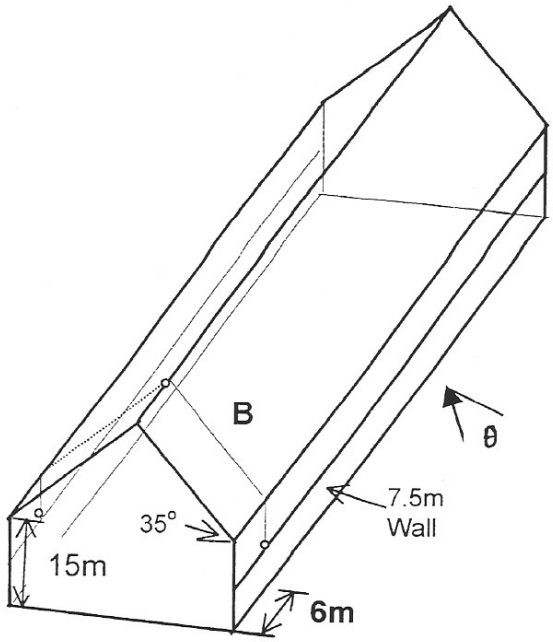

Fig 1. Building Configuration No. 1, span = 40m, height = 29m, AR= 2.4, 4 and 6, $\alpha = 35°$

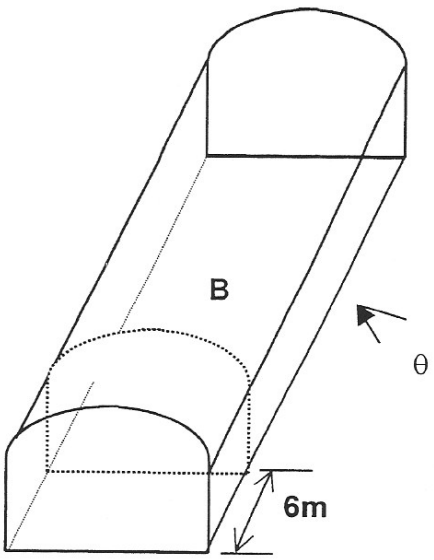

Fig 3. Building Configuration No. 3, span = 45m, height = 29m, AR= 2.4, 5 and 8, Curved Roof

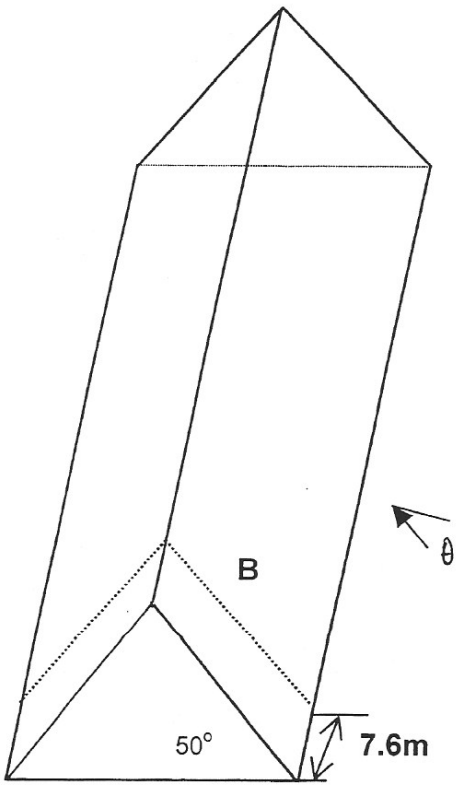

Fig 2. Building Configuration No. 2, span = 50m, height = 30m, AR= 3, 4, 5, 6, 7 and 8, $\alpha = 50°$

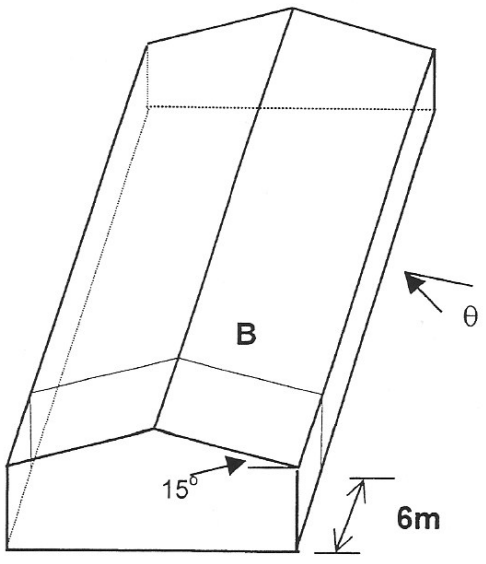

Fig 4. Building Configuration No. 4, span = 80m, height = 26m, AR= 1.35, 3 and 4.35, $\alpha = 15°$

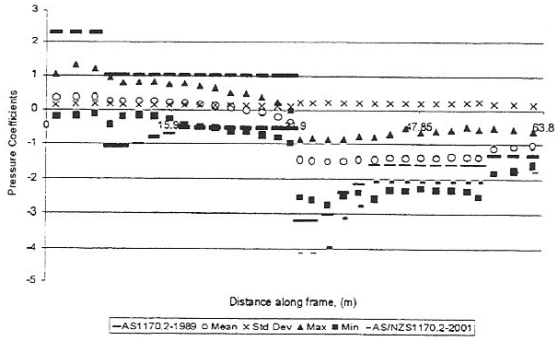

Fig 5. Mean, standard deviation, maximum and minimum *Cps* on Frame B of Building Configuration No. 1, AR = 6, θ = 45°, and AS1170.2 C_{peak} θ = 0°.

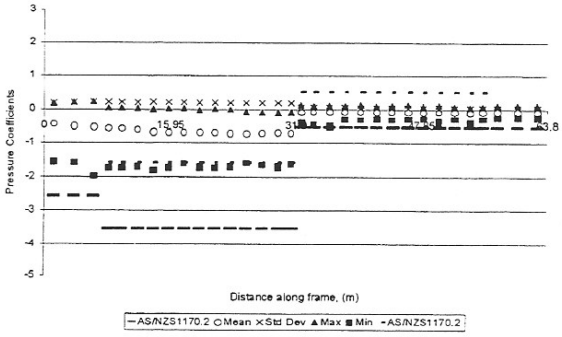

Fig 6. Mean, standard deviation, maximum and minimum *Cps* on Frame B of Building Configuration No. 1, AR = 4, θ = 90° and -90°, and AS1170.2 C_{peak} θ = 90°.

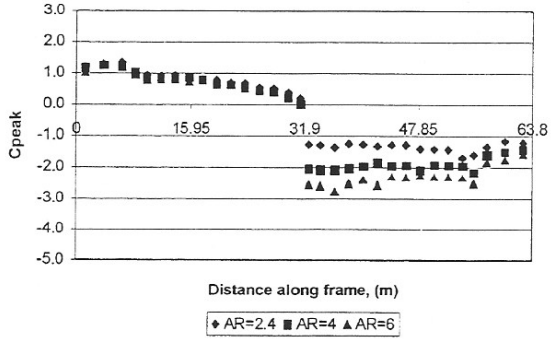

Fig 7. Peak positive and peak negative *Cps* on windward and leeward halves of Frame B on Building Configuration No. 1, θ = 45°

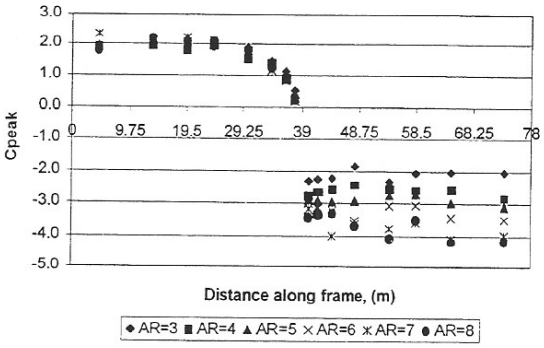

Fig 8. Peak positive and peak negative *Cps* on windward and leeward halves of Frame B on Building Configuration No. 2, θ = 45°

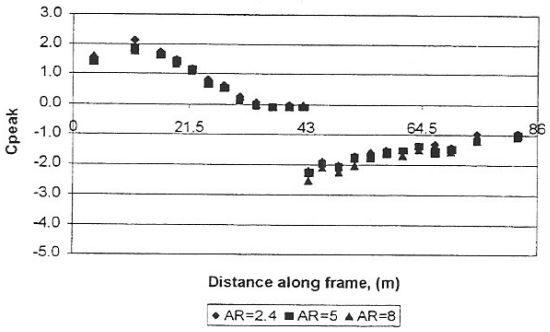

Fig 9. Peak positive and peak negative *Cps* on windward and leeward halves of Frame B on Building Configuration No. 3, θ = 45°

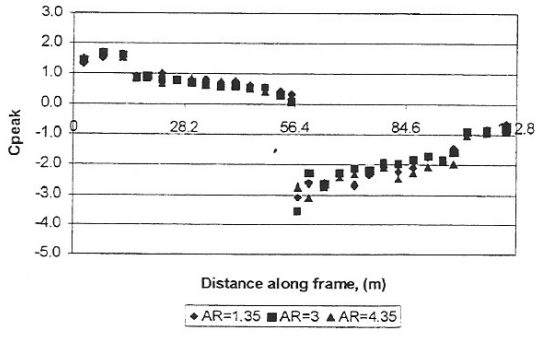

Fig 10. Peak positive and peak negative *Cps* on windward and leeward halves of Frame B on Building Configuration No. 4, θ = 45°